Exploring Inversion Solution Space:
A case study over a Cu-Ag deposit in the Kalahari copper belt

Rob Ellis*
Geosoft Inc.
Toronto ON Canada
robert.ellis@geosoft.com

Cas Lotter
Spectral Geophysics
Cape Town South Africa
cas@spectralgeophysics.com

Taronish Pithawala
Geosoft Inc.
Toronto ON Canada
taronish.pithawala@geosoft.com

SUMMARY

Exploring inversion solution space is the process of mapping out the domain of inversion models which have a predicted response in satisfactory agreement with the observed data. This is particularly important in mineral exploration geophysics because the associated inverse problems are highly ill-posed. An inversion case study over a Cu-Ag deposit in the Kalahari copper belt provides a good demonstration of the process: in the case study 3D IP field data show a clear indication of chargeability so it is no surprise that a chargeability anomaly is recovered from a standard 3D IP inversion. Extensive drilling delineated a disseminated sulphide zone however the drilling delineates a shallow target while the inversion indicates an interesting deeper target. The immediate exploration question is whether to invest in a deep drillhole to test the deeper target? Or is the deeper target merely an artefact of non-uniqueness associated with the IP method?

Exploring the inversion solution space produces a suite of models all of which fit the data satisfactorily. In particular, exploring the solution depth produces a suite of models with a variety of depths, including some models with a shallow chargeability anomaly. This significantly weakens expectations associated with the initial deep inversion model but improves exploration decision making.

Exploring inversion solution space is achieved computationally by systematically modifying the regularization term in the traditional Tikhonov formulation. With an inversion workbench the process is easy, the results are remarkably helpful, and the outcomes surprisingly quickly become a natural part of the exploration team's interpretation process.

Key words: inversion, non-uniqueness, DC, IP, 3D, Kalahari, exploring inversion solution space

INTRODUCTION

It is common practice in mineral exploration to use inversion in an effort to extract the maximum value from geophysical data however as every geophysicist knows there are many earth models with a response in agreement with any given survey dataset. For brevity, we will refer to such models as being *data-equivalent*. It immediately follows that producing a single data-equivalent model in an inversion is not extracting maximum value from the data. There have been continuing efforts from the early days of geophysical inversion to provide some characterisation of the domain of data-equivalent models including optimally localized averages (e.g. Backus & Gilbert, 1970), Bayesian approaches (e.g. Tarantola and Valette, 1982), MCMC methods (e.g. Oh and Kwon, 2001), etc. which can be found described in many excellent texts on geophysical inversion (e.g. Menke, 1984, Tarantola 1987, Zhdanov 2002). Such methods are powerful, elegant and general; however they are often not available to practicing exploration geophysicists. In this work we present a simpler, perhaps more intuitive and more geological approach, to the problem of mapping the domain of equivalent models. We refer to this simpler approach as *exploring inversion solution space*.

We emphasize the *exploring inversion solution space* approach in the hope that it may help practicing geophysicists because in spite of some excellent inversion success stories in the literature and geophysical folk lore, unfortunately, easy inversion successes are rare in the real world and ambiguity and confusion are more often the result. Therefore, in this work we break with tradition and present an inversion case study that produced challenging results: the inversion model does not match geological expectations.

The case study involves an IP survey conducted in the Kalahari Copper Belt as part of a Cu-Ag exploration program. The apparent chargeability field data show a clear indication of a chargeable zone so it is no surprise that a chargeability anomaly is recovered from a standard 3D IP inversion. Extensive drilling delineated a disseminated sulphide zone however this is not a traditional inversion success story; instead ambiguity and confusion arise because the drilling delineates a shallow target while the inversion indicates a deeper target. The immediate exploration question is whether to invest in a deep drillhole to test the deeper target, or is the deep target merely an artefact of non-uniqueness associated with the IP method?

The following sections attempt to briefly convey some of the non-uniqueness inherent to IP inversion and to show that the deep target from the standard inversion is only one of many data-equivalent models and that by simple procedures a suite of models can be generated which provide a much better understanding of what information the IP data truly convey. As a result of our analysis we are still left with some inversion ambiguity however the exploration geophysicist is now in a much better position to set appropriate expectations and to plan subsequent follow up.

The Project

The Kalahari Copper Belt (KCB) of Botswana is a vast region hosting a number of proven shallow economical Cu-Ag sediment hosted disseminated sulphide deposits that are well suited to IP exploration. This case study focuses on the recently defined MOD Resources Cu-Ag T3 Dome Project in the centre of the Kalahari Copper Belt (Figure 1). A description of the deposit and mineralization environment can be found in Catterall et al (2012) and Ellis et al (2017). In brief, the Cu-Ag mineralisation occurs primarily at the redox

interface between oxidising red sandstones and reducing carbonates and shales formations with the highest grades associated with structurally controlled veining. The mineralised package consists of an upper zone of pyrite-sphalerite-galena, a middle zone of bornite-chalcopyrite-pyrite and a lower zone of bornite-chalcosite. The upper zone mineralisation occurs as disseminations tending to clusters and aggregates in cleavages, fractures and veins in the lower zone. Published mineral resources for the Copper Belt have typical grades of 1-2% and 10-30g/t for copper and silver, respectively (from Porter Geoconsultancy Database, 2012).

Figure 1: The location of the T3 Dome Project in the KCB, Botswana.

The Mod Resources tenement under investigation in this study is directly along strike of a thrust-faulted, anticlinal dome with Ngwako Pan Red Beds at its core (Remote Exploration Services, 2012) (Figure 2). The dome is referred to as the Banana Zone and has been relatively well explored, including with 2D IP surveys.

The MOD T3 Dome discovery hole was drilled on a XRF analysed, geochemical soil anomaly (Mod Resources UK Investor presentation, April 2016) some 30km to the south-west of the Banana Zone. From there the drilling was stepped out across and along strike on a 100m square grid and a 50m square grid in places over an area of 800m by 350m (Hanna, 2016).

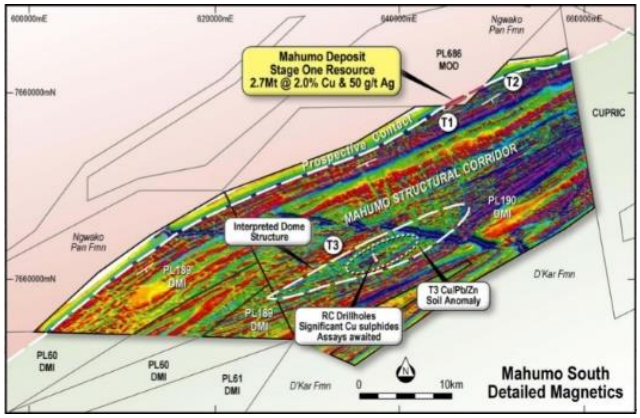

Figure 2: RTP magnetics over the T3 Dome project to illustrate structural controls.

DC IP 2D Inversions

A number of companies, including but not limited to, Anglo American Corporation, Hana Mining, Cupric Canyon Capital and MOD Resources, have conducted IP surveys over various sections of the KCB using primarily 2D arrays. During the T3 Dome drilling program in 2016, a regional forward and reverse pole-dipole array survey was conducted through the centre of the drilling grid over a traverse length of 5km. The dipole length was 200m and useable, maximum n-spacing, varied from 8 to 11. The 2D electrode layout (blue) over the mineralization is shown in Figure 3.

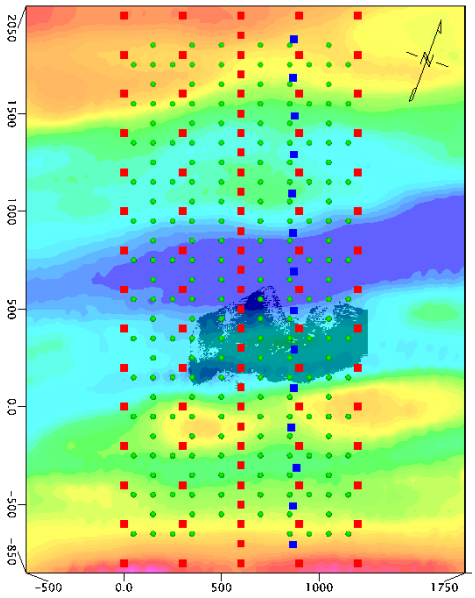

Figure 3: A portion of T3 Dome Cu-Ag resource (black) with sparse 3D array (currents red squares, potentials green circles) and the 2D pole-dipole array (blue squares) on the RTP magnetics.

Figure 4 shows the derived unconstrained conductivity and chargeability models for a data misfit of 1% and with 0.01 mV minimum for the DC inversion and 2 mV/V for the IP inversion. The conductivity model (Figure 4a) shows a series of near surface anomalies, which we interpret to be the inversion manifestation of the conductive Kalahari cover. The sub-cropping T3 deposit is not directly imaged in the conductivity model, possibly being masked by the conductivity cover DC response; however it sits above a well-defined chargeable zone (Figure 4b).

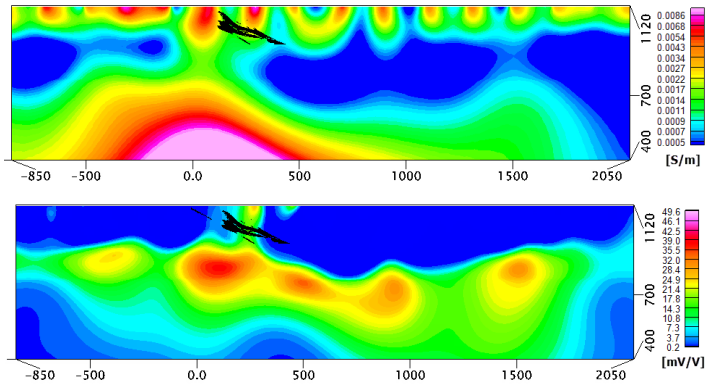

Figure 4. (a: upper) Conductivity and chargeability (b: lower) derived from the 200m pole-dipole array survey with 2D unconstrained inversion with the mineralization for reference (black).

The dip of the chargeable zone is consistent with the T3 Dome resource dip, but the depth to the centre of the body is over-estimated at 300m. Due to the 2D nature of the data, the location of the deeper sources with relation to the line could not be ascertained. Two 500m drill holes on and near the survey line, both missed the intended deep target.

DC IP Sparse 3D Survey

To follow up on the 2D DC IP results a sparse array 3D IP survey was conducted by Mod Resources during the first 2 months of 2017, a first for the KCB. Spectral Geophysics, a consulting and contracting company based in Gaborone, Botswana, conducted the survey consisting of a number of overlapping sparse electrode layouts in a 3D IP configuration. The sparse arrays were design to efficiently cover the T3 Dome deposit, approximately 70km north-east of the town of Ghanzi, with extensions to the south-east and north-west. The proposed layout was implemented over an area measuring approximately 4.5km by 1.2km, using commercially available 3D IP equipment from IRIS Instruments of L'Orleans, France. A subset of the layout over the T3 mineralization is shown in Figure 3 (red and green).

Sparse Electrode Layout 3D IP setup

The 3D IP array consisted of a combination of a quasi-3D linear setup (using an off-set pole-dipole configuration) through the centre of the project area augmented by 20 two channel IRIS Full-Wavers using orthogonal dipoles – one set perpendicular and the other parallel to strike, respectively. The placement of the electrodes relative to the modelled resource and the magnetic field is presented in Figure 3. The Wavers were placed 200m apart, each connected to two orthogonal 100m dipoles. Five overlapping grids were surveyed to create the full data coverage. The infinite was off to the south-west approximately 5km from the edge of the survey area.

The quasi-3D data was collected in asynchronous mode, using two 8 channel IRIS Elrec PRO10 receivers on 2 lines located 100m towards the south-west and north-east of the central transmitting line, respectively. Current injections along the centre line of the survey block were at 100m intervals and elsewhere at 300m intervals. Simultaneously, the 20 Full-Wavers recorded data in synchronous mode using the GPS 1pps signal. Recording time was approximately 300 seconds per current injection for the Full-wavers and 50 stacks for the PRO10s. Current injections were done sequentially, taking care that the current cables were at least 50m clear of receiving dipoles. A total of 42 current transmissions were performed per grid. Pre- and post-processing of the raw field data were done separately for the 2 types of equipment and only merged for modelling purposes.

Quality Control

Rigorous QC was applied to the data checking for null coupling and reversed polarities of primary voltages in particular and monitoring data ranges in general. Noisy readings and suspicious looking decays were deleted, as were data with near-null coupling. Large geometric factors due to long offsets coupled with very low primary voltages were also carefully vetted before including the reading in the final database. The average value of the chargeability over the time interval 0.48 to 1.12 milliseconds was calculated with normalisation by window width.

Plots of the calculated apparent conductivity and average apparent chargeability values are shown in Figures 5a and 5b with respect to the mineral resource. The images are the 3D equivalent of pseudo sections where the plot depth is half the separation between the current electrode and the centre of the potential dipole. Note that the apparent conductivity indicates a surficial conductive layer which we interpret to be due the Kalahari cover and that there is a trend toward slightly higher conductivities in the vicinity of the mineralization and toward the south, however, the range of apparent conductivities is rather limited: 0.2 mS/m to 5 mS/m. The apparent chargeability shows a more convincing association with the mineralization: a 20 mV/V anomaly.

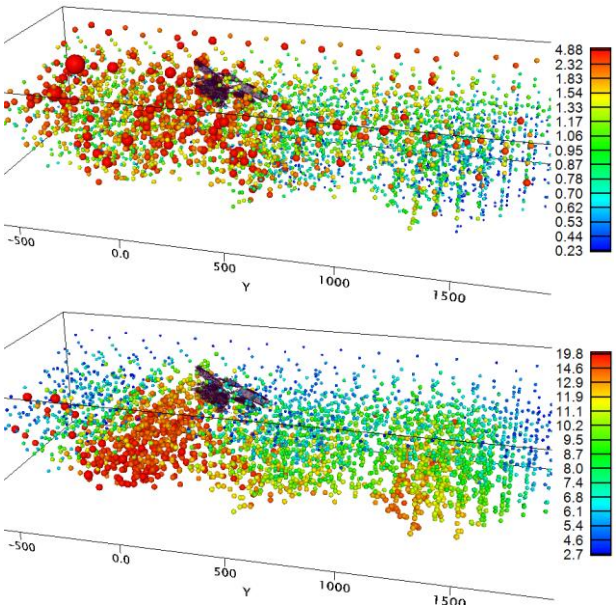

Figure 5: The Ghanzi apparent conductivity (upper, in mS/m) and apparent chargeability (lower, mV/V) data. The known Cu-Ag mineralization is shown in black.

As a practical aside, we emphasize that it is essential to very carefully examine DCIP data before inversion. This is often difficult in practice with 3D data however colour and size controlled symbols with a variety of stretches prove to be effective for identifying outliers and understanding the behaviour of the data, as shown in Figure 5.

METHOD AND RESULTS

All ill-posed inversions require some form of regularization and in this work Tikhonov regularization is used. In the traditional formulation (e.g. Zhdanov, 2002), if the forward problem is written in terms of the model m and the data d as

$$Gm = d$$

then the corresponding inverse problem can be solved by minimizing the (multi-term) parametric functional

$$P^{\lambda}(m,d) = \left\|W_d\left(Gm - d^{\text{obs}}\right)\right\|^2 + \lambda\|W_m(m - m^*)\|^2 + \cdots$$

where W_d and W_m are mathematically arbitrary but are usually chosen to be the data and model covariance respectively. The regularization parameter λ is chosen so that an appropriate data misfit is achieved but otherwise the (often multi-term) regularization is at the user's discretion. By default we choose the regularization to contain terms that promote a smoothly varying model and include an integrated sensitivity factor that promotes the correct recovery of compact spheroidal targets. Any specific requirements on the solution can be added to the default regularization (e.g., parameter bounds, etc.)

Regarding the geophysical IP operator G, while there are several numerical representations for the IP response, in this work we choose the Seigel (1959) representation without loss of generality.

Default 3D DC Inversion

After rigorous QC a "default" DC inversion was performed to produce a conductivity model with voxel elements 12.5m x 12.5m x 6.25m and achieving a 1% with 1mV minimum fit to the data. A conductivity section through the model at X=870m (i.e. under the 2D line) is shown in Figure 6 with the known mineralization in black. The inversion shows a large diffuse conductivity domain under and south of the mineralization but there is little to indicate the presence of a conductivity anomaly associated with the mineralization. The collection of small near surface highs is interpreted to be a manifestation of the conductive Kalahari sand cover. The 3D inversion conductivity section compares reasonably to the 2D pole-dipole DC inversion in Figure 4

A visual representation of the typical fit to the data is shown in Figure 7a, b for the FullWaver and Pro10 data: the fit is extremely good, possibly over fitting. A less stringent data fit results in a more continuous representation of the Kalahari cover; however our aim was determine if the mineralization could be localized so we persist with the more stringent fit.

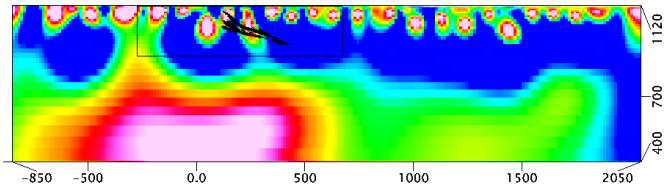

Figure 6: The conductivity section at X=870m for the full data from Blocks 1, 2, and 4 as shown in Figure 3. The known mineralization is shown in black with the black rectangle outlining a smaller domain investigated in more detail subsequently. The colour scale is S/m.

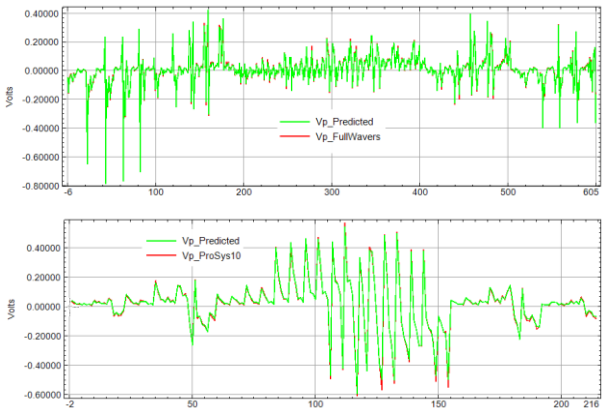

Figure 7: (a, upper) the observed FullWaver (red) and predicted response from the model (green); (b, lower) the observed Pro10 (red) and predicted response from the model (green). The abscissa axis is measurement number.

Default 3D IP Inversion

Using the default conductivity model we performed a default IP inversion with the same model discretization and fitting the IP data to 0.5mV/V. The result for the X=870m section is shown in Figure 8. Again, like the conductivity inversion, there is an indication of a chargeability anomaly under and to the south of the mineralization but very little in the chargeability model that appears to be directly related to the mineralization.

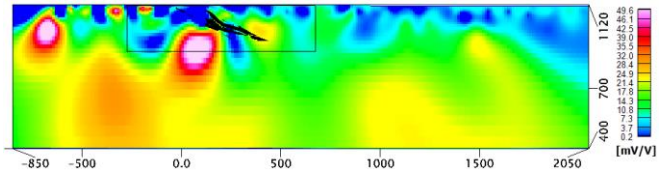

Figure 8: The chargeability section at X=870m for the full data from Blocks 1, 2, and 4 as shown in Figure 3. The known mineralization is shown in black with the black rectangle outlining a smaller domain investigated in more detail subsequently. The colour scale is S/m.

Figures 9a and 9b show typical data fits for the Full-Waver and Pro10 IP data respectively. The fit is reasonable; forcing a better fit generated excessively noisy models.

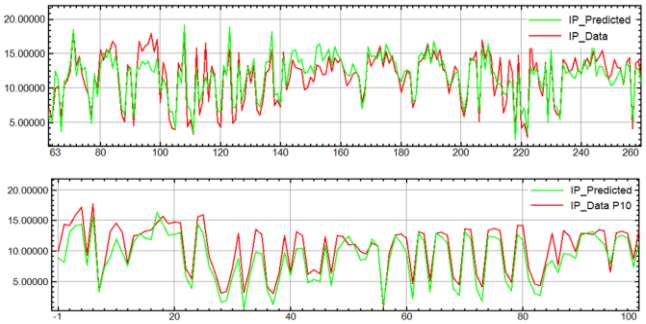

Figure 9: (a, upper) the observed FullWaver (red) and predicted response from the model (green); (b, lower) the observed Pro10 (red) and predicted response from the model (green). The abscissa is measurement number and the ordinate axis is in mV/V.

Thus far, default 3D conductivity and chargeability inversions have been performed and the recovered models appear to be rather indirectly related to the known shallow mineralization. It is exceedingly tempting to become discouraged and conclude that 2D or 3D inversion of the DC IP survey data cannot add significant value to this exploration problem, but let us remember that these results are only one inversion result from an ensemble of data-equivalent conductivity and chargeability models. To improve the value of inversion we must explore the inversion solution space which is the focus in the following Sections.

Numerical Modelling - Validation

It is appropriate at this stage to emphasize that reconciling inversion results with drilling is an extraordinarily difficult problem and includes effects ranging from the detailed petrophysics (dissemination vs veining, etc.) to geophysical non-uniqueness. In this work we choose to focus only on the latter end of this spectrum and investigate whether the inversion results can be reconciled with the drilling data. We approach this by addressing the following two questions: first, is the numerical modelling accurate in this situation; and second, can we show by exploring inversion solution space that there is a geophysical equivalence between a shallow layer and a deeper target?

We begin with a simple test for numerical accuracy: computing the 3D finite volume (FV) response over a layered earth and comparing with the quasi-analytic (QA) 1D response (e.g. Keller and Frischknecht, 1966). A 1D model is chosen for comparison because the mineralization is thin, sheet-like, and dips at approximately 30°. In particular, we must

determine the FV discretization required to accurately represent a thin sheet. This test is essential to ensure that the deeper target is not merely a result of erroneous modelling of a shallow target.

In Figure 10 the apparent resistivity for the QA response is shown (solid black) for a 5m thick 1Ωm layer starting at 20m in a 1000Ωm host. The QA response for a 100m thick 20Ωm layer also starting at 20m is shown in black triangles demonstrating the well-known layer conductance equivalence. The numerical responses from the FV algorithm with 1x5m, 2x2.5m and 4x1.25m thick cells simulating the layer are shown as blue, red, and green respectively. In all cases the VOXI-DCIP FV algorithm gives an accurate response. It is perhaps surprising to observe that only a single layer of FV cells is required to accurately represent the true horizontal layer. Since the Ghanzi mineralization is dipping we propose that using 3-4 cells in thickness to simulate the anomalous conductivity and chargeability should provide sufficiently accurate forward modelling. As an aside, this QA-FV comparison also confirms that the numerical boundary conditions are sufficiently satisfied: an important check for any modelling.

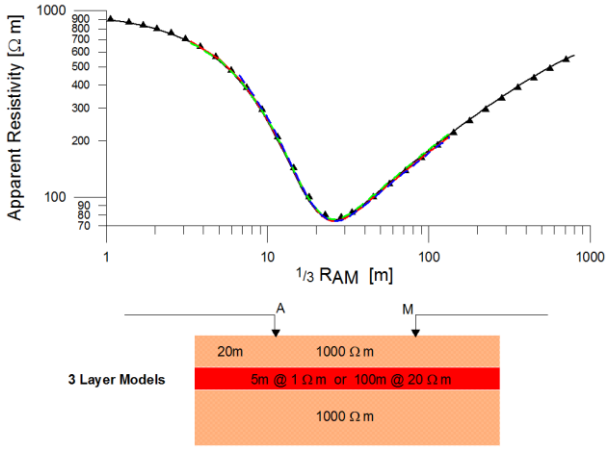

Figure 10: The apparent resistivity as a function of pole-pole separation over a 3 layer model. The quasi-analytic response is shown in solid black for 5m thick 1 Ωm layer at 20m in a 1000 Ωm host. The FV response is shown as blue, red, and green for different layer vertical discretizations. See the text for a full description.

Other numerical validations can be found elsewhere (Ellis, 2018) based on the QA responses over quarter spaces and a buried sphere.

Numerical Modelling – Setting Expectations

It is instructive to invert the 1D response shown in Figure 10 with a standard smooth 1D inversion in order to set expectations on subsequent inversions of 3D synthetic and field data. Choosing to fit the data to 5% the inversion produces a smooth model that has a broad conductivity maximum at ~80m as shown in Figure 11. Also shown is the 100m thick 20 Ωm data-equivalent model.

Figure 12 shows the corresponding smooth with positivity chargeability inversion result analogous to the conductivity result in Figure 11. To generate the synthetic IP data the intrinsic chargeability of the layer was chosen to be 0.5 for a 5m layer below 20m depth (black), coincident with the 1 Ωm layer used in the DC case. For the inversion the base conductivity model was taken from smooth DC inversion (i.e. Figure 11, blue). The resulting smooth chargeability (Figure 12, blue) shows a very broad and deep chargeable zone.

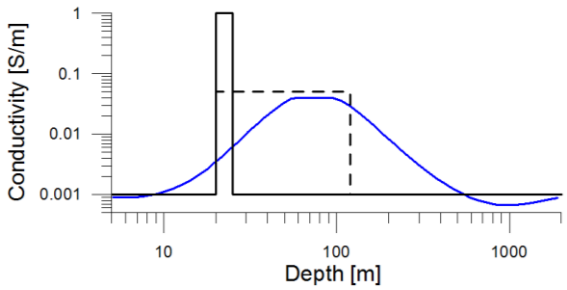

Figure 11: The 1D smooth inversion conductivity (blue) from data generated by either of the equivalent 3 layer models starting at 20m depth and having vertical conductance 5 S (black).

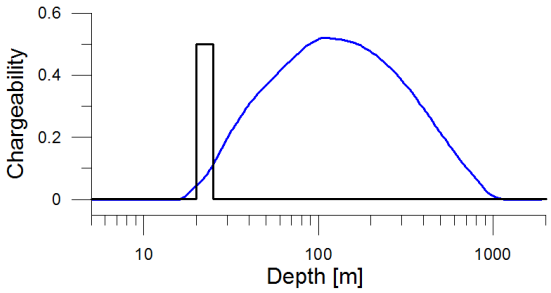

Figure 12: The 1D smooth inversion chargeability model (blue) from apparent chargeability data generated by the 5m 0.5 chargeability layer starting at 20m depth (black).

This simple 1D inversion demonstrates that we should expect the *default* smooth DC and IP 3D inversion of the Ghanzi mineralization to generate a model that is smooth and located below the thin dipping Cu mineralization.

Synthetic Model Test

We can refine our expectations at Ghanzi T3 by creating a 3D synthetic conductivity model based on the observed Cu mineralization then simulating and inverting the DC response based on the Ghanzi survey layout. The forward model was discretised onto a 2m mesh to minimize any discretization errors in the synthetic DC and IP responses. In order to avoid any favourable bias the inversion was performed on a different 6.25m mesh. An attempt was made to produce the best possible conductivity inversion result model to gauge the best possible outcome from the survey configuration: the synthetic data were fit to 1% or 0.1mV. The result is shown in Figure 13a as a conductivity section at X=450m. The true Cu mineralization is shown in black. The recovered conductivity manifests as a compact target under the dipping sheet of conductivity in agreement with our expectation from 1D modelling. Note that the conductivity anomaly is under the main bulk of the mineralization and that the down dip extension of the target is not recovered at least partly because of the surveys limited n-spacing.

Figure 13b shows the corresponding chargeability section at X=450m achieved with a data misfit of 5 mV/V, which corresponds to approximately 1% of the data maximum. Like the conductivity, the recovered chargeability manifests as a compact dipping target under the true target as expected from the 1D case.

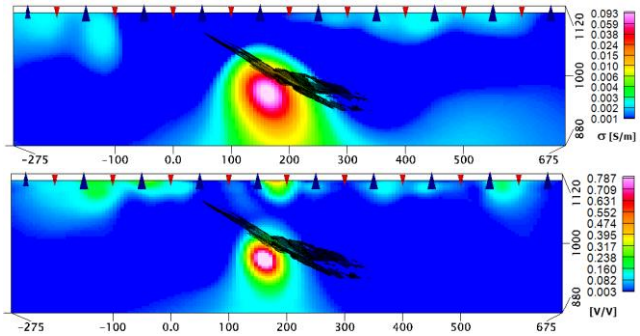

Figure 13: (a, upper) A section through the default inversion conductivity model; (b, lower) the corresponding default chargeability section. The true model is shown in black.

Exploring Inversion Solution Space

The deep inversion models shown in Figure 13 are only one realization of all data-equivalent models. We can provide a more comprehensive and more satisfying inversion result by *exploring inversion solution space*: that is, by varying the implicit and explicit constraints in the inversion process to produce a variety of models which begin to provide a deeper understanding of what information is truly contained in the data. The inversion solution space can be mapped out by varying the Tikhonov regularization term. A simple and effective approach is add an extra operator W_e to the traditional formulation

$$P^{\lambda}(m,d) = \left\|W_d\left(Gm - d^{\text{obs}}\right)\right\|^2 + \lambda\|W_m W_e(m - m^*)\|^2 + \ldots$$

For example, to explore inversion solution space in depth z set $W_e = diag(f(z))$ and to promote a shallow solution $f(z) \sim z$. Using different functional forms $f(z)$ generates a map of the depth of data-equivalent anomalies. Although this modification is simple, in practice, it works extremely effectively.

In the synthetic example above, the default inversion recovered a default model with the chargeability anomaly too deep. In our synthetic case we know the true model and therefore realize that the default inversion model must be data-equivalent to the true model. In an exploration context where the true model is unknown the issue becomes: how confident should the exploration team be in the target depth indicated by the inversion, or, what is the domain of (plausible) data-equivalent models?

We can map out some useful information about the domain of data-equivalent models in depth by varying the Tikhonov regularization term with results shown in Figure 14 (top to bottom for shallower to deeper solutions). For example, in Figure 14b $f(z) \sim z$ factor has been applied and the depth of the recovered anomaly now lies exactly on the true model. Of course, while this depth match is interesting it is no more or less meaningful than the default solution. In Figure 14d we show the subdomain of plausible data-equivalent solutions we have recovered from exploring the inversion solution space: the data support a chargeability anomaly from at least 50 m to 150m.

The preceding chargeability inversions were intentionally performed with a rather stringent data misfit of approximately 1% of the data maximum (5 mV/V) in order to illustrate the domain of data-equivalent models with almost perfect fit to the data. In practice, only a less stringent fit to the data is usually possible. To illustrate the effect on the domain of data-equivalent models induced by significantly increasing the IP error levels we show the equivalent of Figure 14d but with an increased data misfit of approximately 7% of the data maximum (30 mV/V). As expected the anomaly becomes significantly less compact and with lower amplitude. Importantly, the apparent depth of the chargeability target is independent of error level for practical purposes.

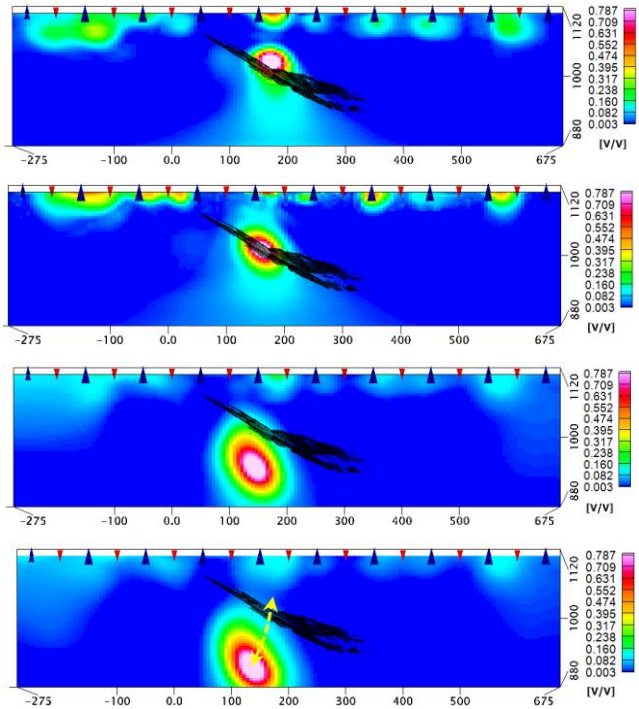

Figure 14 (a-d, top to bottom): Exploring inversion solution space in the depth direction for the default chargeability inversion in Figure 13b. As the series progresses from top to bottom the z-dependence drives the data-equivalent solutions from shallower to deeper. All models have the same data fit. The true model is shown in black and the yellow arrow indicates the migration of the recovered anomaly with z regularization dependence.

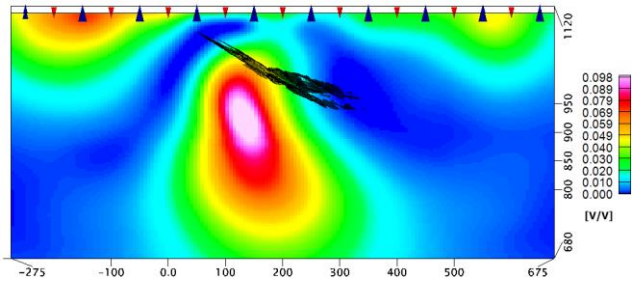

Figure 15: Exploring inversion solution space as the recovered model data fit is increased to 30mV/V, c.f. Figure 14d.

Exploring Inversion Solution Space – Ghanzi T3 Survey

The preceding synthetic example strongly suggests that the deep chargeable target recovered from the default inversion of the Ghanzi T3 data should not be treated as a sine qua non. Therefore, we return to the Ghanzi survey and explore the inversion solution space. For expediency and clarity we localize our study to a smaller domain around the known mineralization, extending from Y= [-275, 675] and concentrate on sections at X=450m. Figure 16 shows the results of the default conductivity and chargeability inversion

at this smaller scale (corresponding to the smaller black rectangle in Figures 6 and 8).

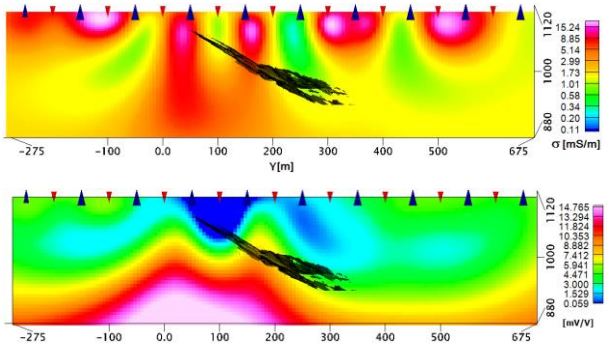

Figure 16: (a, upper) A section through the default conductivity inversion model at X=450m; (b, lower) the corresponding default chargeability inversion. The known mineralization is shown in black.

Recall that the exploration question at Ghanzi is whether there is truly a deep chargeable target which warrants further expensive drilling, or, is the default deep chargeability anomaly data-equivalent to a shallower model more consistent with the already known mineralization? Exploring the inversion solution space in the direction of shallower targets yields the results shown in Figure 17 (a-c): Figure 17a shows the default inversion; Figure 17b shows the result of using a depth factor proportional to z while Figure 17c shows the result for a z^2 dependent depth factor. We see the deep target rises from a depth of approximately 300m to a depth of approximately 100m significantly altering the initial interpretation based on a default inversion model.

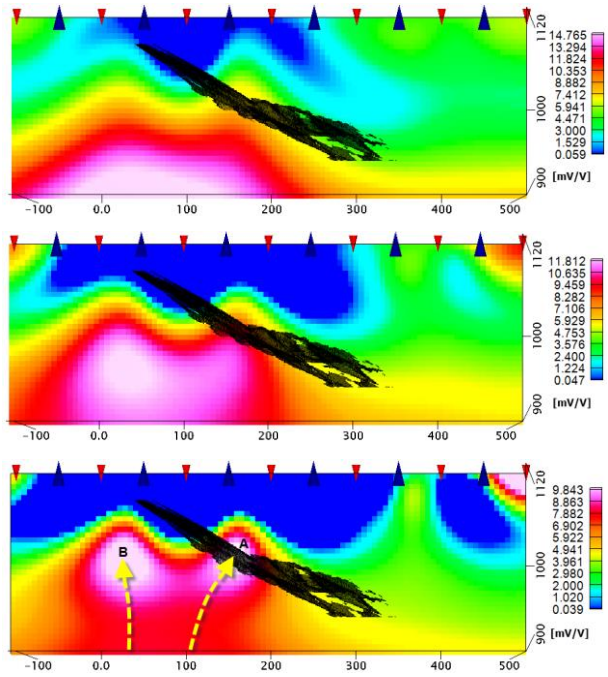

Figure 17: (a, upper) A section at X=450 through the default chargeability inversion for the Ghanzi IP data; (b middle) the same section with a z-dependent regularization factor; (c, lower) with a z^2-dependent weighting. The known mineralization is shown in black. The yellow arrows indicate the migration of the recovered anomaly with z regularization dependence.

The shallower Ghanzi inversion result in Figure 17c mirrors one aspect of the behaviour observed with the synthetic test and in doing so it strongly suggests that the domain of data-equivalent chargeability models can include a component (denoted by A) consistent with the known mineralization (c.f. Figure 14b). However there is an additional component (denoted by B) which requires further investigation and is the focus of ongoing work.

CONCLUSIONS

A non-traditional inversion case study has been presented in which the default inversion model and the ground truth appear inconsistent, a rather common occurrence in real world mineral exploration geophysics. The apparent disparity motivated the process of *exploring inversion solution space*, a process where the domain of *data-equivalent* models is mapped by varying the Tikhonov regularization. In particular, the focus was on mapping inversion anomaly depth. Exploring inversion solution space is a practical, effective, and interactive approach complementing existing more heavily mathematical methods.

The inversion case study was based on sparse IRIS Full-Waver and ProSys10 3D IP data collected in the KCB over known Cu-Ag mineralization. It was initially expected that IP inversion would resolve the known disseminated metallic sulphides, however, that expectation was not supported by the default inversion results. Instead a deep strong chargeability source was recovered below and offset from the known mineralization. The exploration question became: should the deep target be followed up with another deep drillhole?

Exploring the inversion solution space demonstrated that a data-equivalent shallower chargeability target is feasible, significantly weakening the case for an interesting additional deeper, chargeable, mineralized zone. Importantly, exploring the inversion solution space produced a suite of data-equivalent models which provided the exploration team with a more realistic set of expectations associated with the geophysical survey than is usually associated with delivering a single default inversion model.

We emphasize that while our case study involved 3D DC IP data and inversion, our results should not be misconstrued to suggest that the DC IP method is particularly non-unique among geophysical methods. *All* mineral exploration methods suffer from non-uniqueness and their interpretation will benefit from exploring inversion solution space.

We conclude with the encouraging observation that after exploring inversion solution space for a number of projects a remarkable change quickly comes over the concept of inversion in the mind of the geoscientist: one stops thinking in terms of "a model" resulting from a geophysical survey but rather in terms of an ensemble of data-equivalent models with particular characteristics.

ACKNOWLEDGMENTS

The authors thank Mod Resources for access to the field data used in this work and we thank Geosoft Inc. for the VOXI Earth Modelling subscription and the flexible tools which make exploring inversion space effective and efficient.

REFERENCES

Backus, G.E., and Gilbert, F. 1970, Uniqueness in the Inversion of inaccurate Gross Earth Data, Philosophical Transactions of the Royal Society of London A, vol. 266, pp. 123–192.

Catterall D., Grant J., Meister S.N., Obiri-Yeboa T., Cresswell M. and Channon W., 2012, Ghanzi Copper-Silver Project, Ghanzi District, Botswana: in NI 43-101 Technical Report, Prepared for Hana Mining Ltd, www.sedar.com, pp. 1-4, 20-32.

Ellis, R. G., Lotter, C., Pithawala, T., 2017, Sparse 3D IP Electrode Array Data and Inversion over a Cu Ag Deposit in the Kalahari Copper Belt: Extended Abstracts SAGA, 15th Biennial Conference.

Ellis, R. G., 2018, Validating the VOXI-DCIP algorithm, Geosoft Inc. www.geosoft.com\technicalreports

Hanna, J., 2016, Exciting new developments in the Kalahari copper belt: Mod Resources and Metal Tiger, Botswana Resource Sector Conference, Gaborone.

Keller, G.V.; Frischknecht, F.C., 1966, Electrical methods in geophysical prospecting: Pergamon.

Menke, W., 1984, Geophysical data analysis: discrete inverse theory: Academic Press Inc.

Oh. S., Kwon, B., 2001, Geostatical approaches to Bayesian inversion of geophysical data: Markov chain Monte Carlo method, Earth Planets Space 53 (8), pp 777-791

Porter Geoconsultancy Database, http://www.portergeo.com.au/database/mineinfo.asp?mineid=mn1481

Remote Exploration Services, 2012, Presentation and interpretation of magnetic data and soil sampling results – Kalahari Copper Belt, Botswana, Private and Confidential report compiled for Discovery Metals Limited.

Seigel, H. O., 1959, Mathematical formulation and type curves for induced polarization: Geophysics, 24, pp. 547-565.

Tarantola A. and Valette B., 1982, Inverse Problems = Quest for Information: Journal of Geophysics, 50, pp. 159-170.

Tarantola, A., 1987, Inverse problem theory: Methods for data fitting and model parameter estimation: Elsevier.

Zhdanov, M.S., 2002, Geophysical Inverse Theory and Regularization Problems: Methods in Geochemistry and Geophysics, 36, Elsevier.

Remote Exploration Services, 2012, Presentation and interpretation of magnetic data and soil sampling results – Kalahari Copper Belt, Botswana, Private and Confidential report compiled for Dicovery Metals Limited.

VOXI Earth Modelling, Geosoft Inc., www.geosoft.com/products/voxi-earth-modelling/overview